LOW-FREQUENCY CHARACTERIZATION OF SWITCHED DC-DC CONVERTERS

G. W. Wester and R. D. Middlebrook

California Institute of Technology
Pasadena, California 91109

ABSTRACT

Averaging techniques are developed here to represent buck, boost, and buck-boost types of switched dc-dc converters by approximate continuous models. Simple analytical expressions in terms of the circuit components are derived for the characteristic transient and frequency responses of time-averaged (continuous) power-stage models for use in designing and understanding the behavior of corresponding switched power stages. Novel conclusions include the dependence of effective circuit component values upon switch duty ratio and the existence of a real positive zero in certain transfer functions. Responses from analog computer simulations of the switched and averaged power stages agree well and, in turn, confirm the analytic predictions. High-order systems can be analyzed by the averaging technique without a commensurate increase in complexity.

INTRODUCTION

Switched dc-dc converters are composed of two functional blocks as shown in Fig. 1: the power stage chops, rectifies, and filters an analog signal derived from the source v_s to produce an analog output voltage v, and the switch controller provides from an analog signal ϵ the digital control d necessary to drive the "chopping" switch in the power stage. Figure 2 shows representative power-stage types (buck, boost, and buck-boost) commonly used in switched converters; the assumed load is resistive R, and resistances R_ℓ and R_c are included to account for parasitic losses exposed by large currents in the physical inductor and capacitor. The nature of circuit operation has been adequately discussed elsewhere (1) and will not be reiterated here. The duty ratio D, defined as the fraction of time that the chopping switch is closed, is a control mechanism for varying the dc output voltage. One can assume without loss of generality that the switch is driven by the digital signal d according to

$$d(t) = \begin{cases} 1, & \text{switch closed} \\ 0, & \text{switch open} \end{cases} ; \qquad (1)$$

consequently, D is numerically equal to the dc average of $d(t)$.

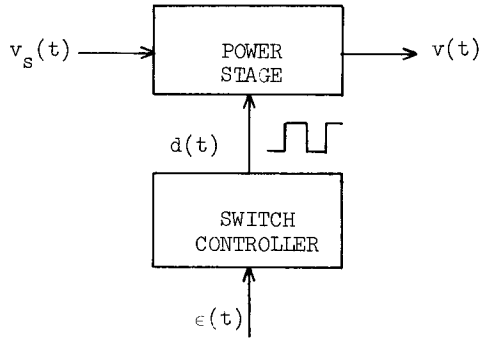

Figure 1. Block diagram of a power stage and controller.

When the converter is part of a regulator in which the controller input ϵ is generated from an appropriate feedback signal, then closed-loop stability becomes important. Stability can be examined if one knows how a disturbance in ϵ propagates through the controller and power stage to affect d and v. A given switch controller can be characterized at least approximately by describing-function analysis, but the power stage, because it is a switched nonlinearity not amenable to conventional analysis, has succumbed only to a static description (2) of the dc output in terms of duty ratio. In review, the static ratio of dc output to dc source input varies with duty ratio and is always less than unity for buck, always greater than unity for boost, and either greater or less than unity for buck-boost power stages.

The present objective is to extend the static description of power stages by analyzing dynamic (e.g. transient and sinusoidal) variations of the two power-stage inputs; in essence, this means finding the effective transfer functions which relate v_s and ϵ to power-stage output v, even though the power stage is switched and nonlinear. Previous attempts at dynamic analysis were either prematurely stalled (3) before reaching simple equivalent circuits and tractable expressions, or thwarted by poor experimental correlation (4). The objective is attained here by the development of continuous linearized models for the switched power stages in Fig. 2; thus, the power stage and controller can be treated as separate linear blocks.

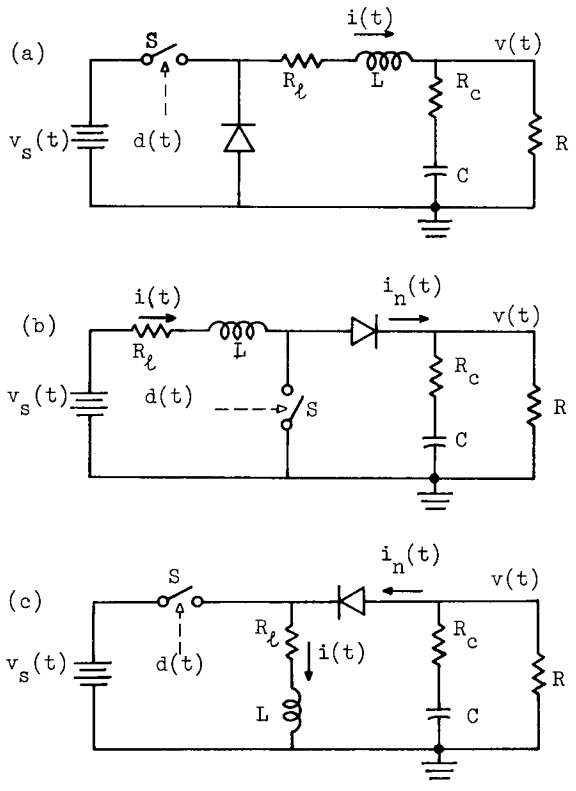

Figure 2. Circuit configurations of switched power stages: (a) buck, (b) boost, and (c) buck-boost.

AVERAGED POWER-STAGE MODELS

General Models

Consider first the boost power stage. One can easily verify that Fig. 3 is an exact equivalent circuit[1] of the boost power stage shown in Fig. 2(b). The factor 1-d(t) can be identified as a discontinuous dependent generator gain and is the principal cause of analytic difficulty. If one is willing to neglect detail in order to study long-range trends, then the forcing functions (sources) may be averaged over a time interval small with respect to the response times of the state variables without appreciably altering the essential nature of circuit response. This concept is the basis of subsequent simplifications; its usefulness arises from the fact that by design the state-variable response times are always much greater than the nominal period T of the switch controller, and therefore the averaging interval can be comparable to the switching period in order to average the factor 1-d. A possible definition of the averaging operation, which is useful for the extraction of low-frequency components from d,

[1]Observe the following notational convention: circles are used to denote independent sources, whereas squares represent dependent generators.

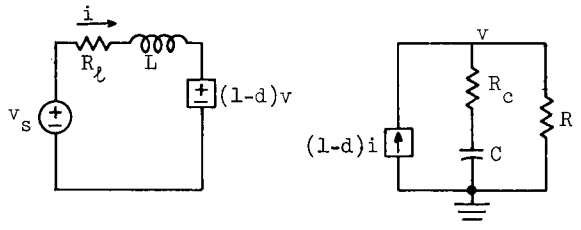

Figure 3. Equivalent circuit of switched boost power stage.

is given (1) by

$$\langle d \rangle(t) = \frac{1}{T} \int_{t-T}^{t} d(x)\, dx \qquad (2)$$

The effect of averaging is approximately that of a low-pass filter with cut-off frequency $\omega_s = 2\pi/T$.

The time-averaged model of the boost power stage is shown in Fig. 4(a). The model is useful only for frequencies less than ω_s since the switching ripple has been averaged out. Although the model is still basically nonlinear, the dependent generator gains are now continuous. In the same manner, averaged models of the buck-boost and buck power stages, respectively, are obtained and illustrated in Figs. 4(b) and 4(c). Because its dependent generator gains are unity, the averaged buck power stage can be simplified to the linear equivalent circuit in Fig. 4(d).

The basic models have now been formulated to analyze the slowly-varying average envelope of power-stage responses. Transient and frequency analysis of the response to the two power-stage inputs, source and control, will be investigated next; however, since super-position does not apply for nonlinear circuits, a particular response is meaningful only if both inputs are specified.

Analysis of Response to Source Variations

Assume for simplicity that the averaged control is constant[2]:

$$\langle d \rangle(t) = D \qquad (3)$$

The equivalent circuit which results when Fig. 4(d) is specialized by the above substitution is shown in Fig. 5 and relates unspecified source variations to the corresponding output variations for the buck power stage. In applying the same procedure to the boost power stage, one can define a complementary duty ratio D' as

$$D' \equiv 1 - D \quad , \qquad (4)$$

[2]As previously noted, that constant is numerically equal to the duty ratio.

which with Eq. (3) and Fig. 4(a) yields the averaged model shown in Fig. 6(a). The dependent generators can be eliminated by normalizing the constant generator gains to unity in the following manner. If in the inductor loop one divides the voltage sources and impedance values by the factor D', the current <i> remains unchanged. After the current generator gain has been similarly normalized to unity, the equivalent circuit shown in Fig. 6(b) can be further simplified to the linear circuit model in Fig. 6(c). Development of the corresponding buck-boost model is entirely analogous to that of the boost model so only the final simplified circuit, which results from the assumption in Eq. (3), is shown in Fig. 7.

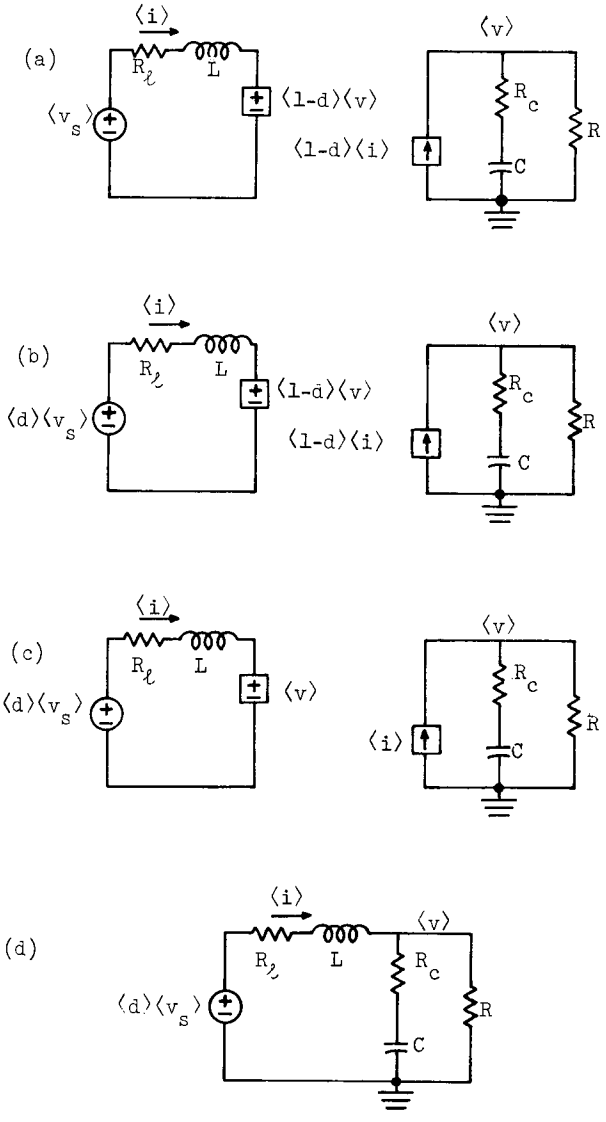

Figure 4. Averaged power-stage models: (a) boost, (b) buck-boost, (c) buck, and (d) simplified buck.

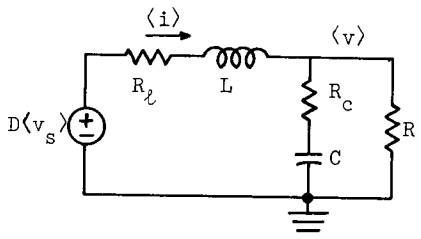

Figure 5. Equivalent circuit of the averaged buck power-stage model for source variations and constant control.

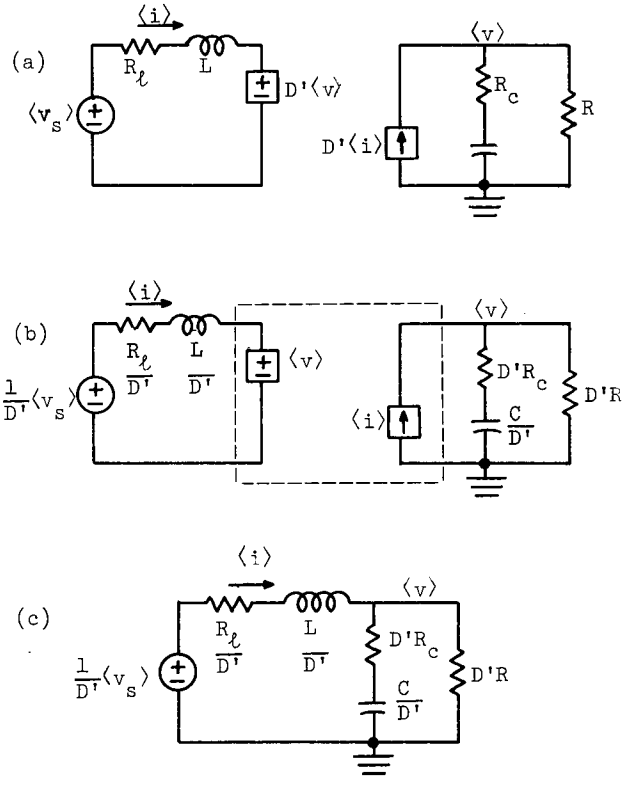

Figure 6. Reduction of the averaged boost power-stage model for source variations and constant control.

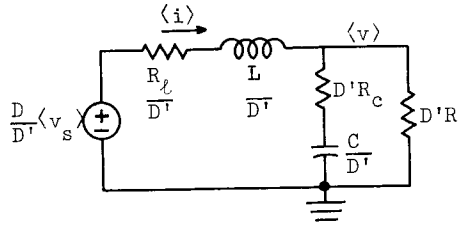

Figure 7. Equivalent circuit of the averaged buck-boost power-stage model for source variations and constant control.

The averaged circuits in Figs. 5, 6(c), and 7 are linear and hence useful for analysis of either transient or frequency responses caused by variations in the source voltage; when the source is held constant, they also apply for transient analysis caused by the control input since the control is constant following a step change. Although the circuit topology for each power-stage type is identical, notice how the effective circuit component values for the boost and buck-boost power stages are modified by the (complementary) duty ratio. When Laplace transform theory is applied to each type of power stage to find the source-input transfer function $G_s(s)$ defined as

$$G_s(s) \equiv \left.\frac{V(s)}{V_s(s)}\right|_{\text{zero initial conditions}} , \qquad (5)$$

where $V(s)$ and $V_s(s)$ are respectively the Laplace transforms of $v(t)$ and $v_s(t)$, the result can be expressed as

$$G_s(s) = A_{so}\, G_f(s) , \qquad (6)$$

where

$$G_f(s) = G_{fo}\frac{1 + \frac{s}{\omega_z}}{1 + \frac{1}{Q}\frac{s}{\omega_o} + \left(\frac{s}{\omega_o}\right)^2} . \qquad (7)$$

Equation (6) can be interpreted as the transfer function of an amplifier in series with a filter as shown in Fig. 8. Analytic expressions for the normalized filter and amplifier factors are listed in Table 1 for each type of power stage; observe the effect of duty ratio on selected corner frequencies and on the quality factor of the filter as a consequence of modified effective component values.

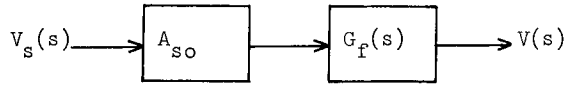

Figure 8. Block diagram of the averaged power-stage model for source variations and constant control.

Analysis of Response to Control Variations

Consider now the situation when the averaged source voltage is a constant V_s,

$$\langle v_s \rangle(t) = V_s , \qquad (8)$$

and the averaged control is fluctuating with time. The buck power stage is readily investigated by using the above substitution in Fig. 4(d) to obtain Fig. 9, which is a linear circuit with constant component values; however, the averaged boost and buck-boost models are nonlinear for variations of the control so a different approach is required.

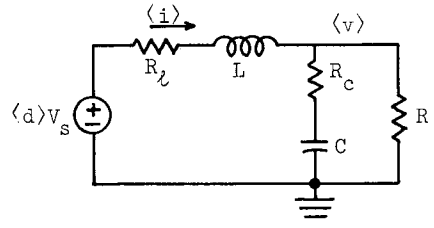

Figure 9. Equivalent circuit of the averaged buck power-stage model for control variations and a constant source.

The transient responses of the various power stages caused by step changes in averaged control are directly available from the equivalent circuits in the preceding subsection when the averaged source is constant, so in the present subsection the effect of an arbitrary control perturbation on the output is sought. Assume the averaged control is given by

$$\langle d \rangle(t) = D + \hat{d}(t) , \qquad (9)$$

where $\hat{d}$ is a time-varying perturbation of the duty ratio D. Based on Eqs. (4) and (9), one can show that

$$\langle 1\text{-}d \rangle(t) = D' - \hat{d}(t) . \qquad (10)$$

The control perturbation causes corresponding perturbations of the averaged state variables as expressed by

$$\langle v \rangle(t) = V + \hat{v}(t) \qquad (11)$$

$$\langle i \rangle(t) = I + \hat{i}(t) . \qquad (12)$$

The problem is to find $\hat{v}$ in terms of $\hat{d}$. The equivalent circuit of the averaged boost power stage which results when Eqs. (8) to (12) are substituted into Fig. 4(a) is shown in Fig. 10(a). After the unperturbed values of the state variables are evaluated from the steady-state equivalent circuit in Fig. 10(b) and subtracted from Fig. 10(a), the equivalent circuit which remains for perturbations is shown in Fig. 10(c). The circuit in Fig. 10(c) can be linearized by restricting the perturbation amplitude in order to make the second-order terms $\hat{d}\hat{v}$ and $\hat{d}\hat{i}$ negligibly small with respect

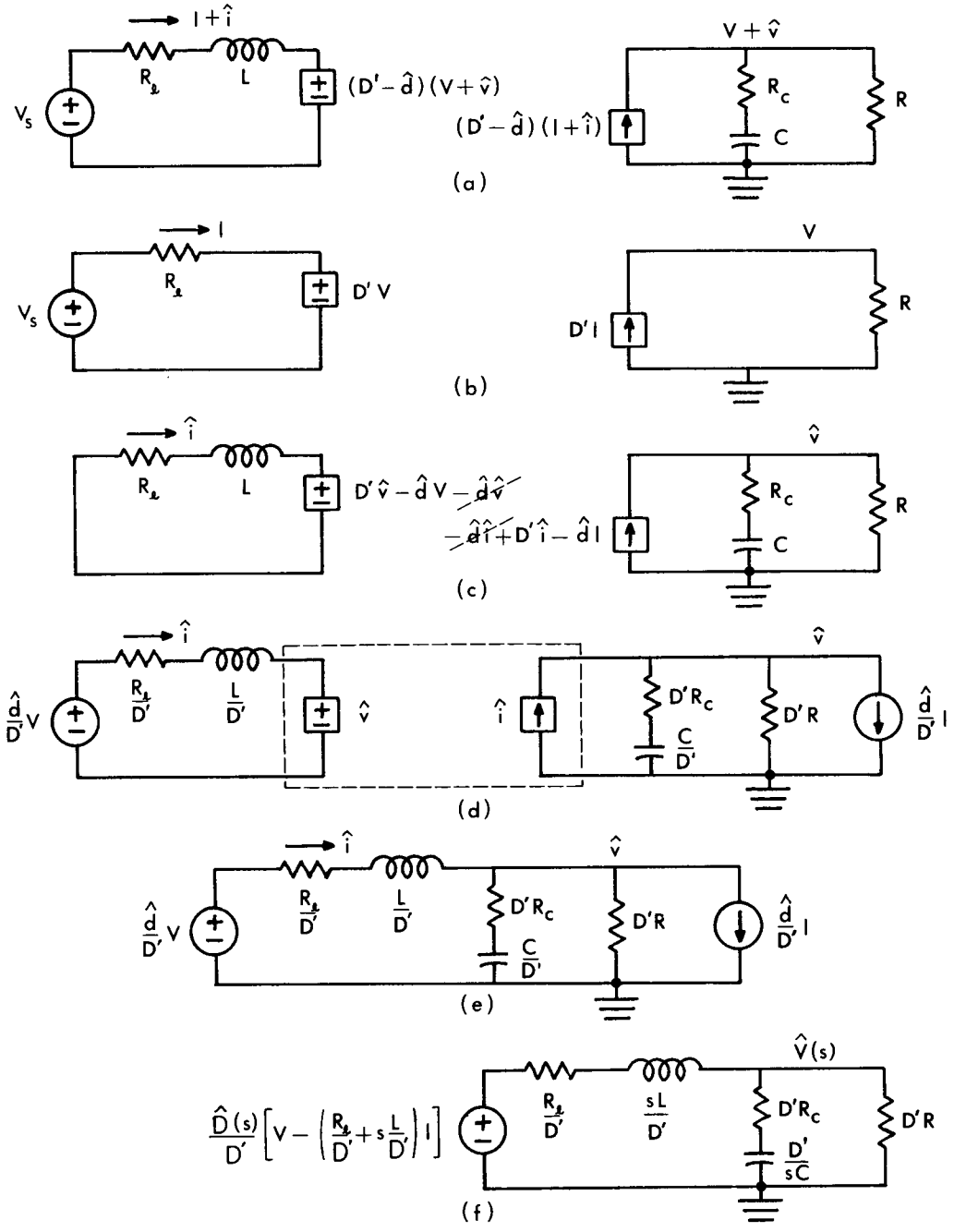

Figure 10. Reduction of the averaged boost power-stage model for small control variations and a constant source.

Table 1. Summary of analytic parameters in power-stage transfer functions.

	Buck	Boost	Buck-Boost
A_{so}	D	$1/D'$	D/D'
A_{co}	V_s	$\frac{(D')^2R - R_\ell}{(D')^2R + R_\ell} \frac{V_s}{(D')^2}$	$\frac{(D')^2R - (D-D')R_\ell}{(D')^2R + R_\ell} \frac{V_s}{(D')^2}$
G_{fo}	$\frac{R}{R + R_\ell}$	$\frac{R}{R+R_\ell/(D')^2}$	$\frac{R}{R+R_\ell/(D')^2}$
ω_o	$\frac{1}{\sqrt{LC}}\sqrt{\frac{R + R_\ell}{R + R_c}}$	$\frac{1}{\sqrt{LC}}\sqrt{\frac{(D')^2R + R_\ell}{R+R_c}}$	$\frac{1}{\sqrt{LC}}\sqrt{\frac{(D')^2R + R_\ell}{R + R_c}}$
Q	$\frac{1}{\omega_o}\left[CR_c + \frac{CRR_\ell + L}{R+R_\ell}\right]^{-1}$	$\frac{1}{\omega_o}\left[CR_c + \frac{CRR_\ell + L}{(D')^2R+ R_\ell}\right]^{-1}$	$\frac{1}{\omega_o}\left[CR_c + \frac{CRR_\ell + L}{(D')^2R+R_\ell}\right]^{-1}$
ω_z	$\frac{1}{CR_c}$	$\frac{1}{CR_c}$	$\frac{1}{CR_c}$
ω_a	∞	$\frac{(D')^2R - R_\ell}{L}$	$\frac{(D')^2R - (D-D')R_\ell}{DL}$

to the other generator terms:

$$\left.\begin{aligned}\hat{v} &\ll V\\ \hat{i} &\ll I\end{aligned}\right\} \text{for small-amplitude } \hat{d} \quad . \qquad (13)$$

For each generator one of the remaining terms is proportional to the independently forced control perturbation while the other is proportional to a circuit-dependent perturbation, so meaningful separations into dependent and independent generators can be accomplished. Following the procedure described in the preceding subsection, one can normalize to unity the gains of the dependent generators to reveal the circuit illustrated in Fig. 10(d). The dotted section of Fig. 10(d) should be recognized as an ideal unity-gain transformer, so it can be simplified as shown in Fig. 10(e). The presence of two generators in Fig. 10(e) obscures the relationship between $\hat{d}$ and $\hat{v}$, but since the circuit is linear, Laplace transforms can be manipulated using Thevenin and Norton equivalents to combine the generators into the single source shown in Fig. 10(f). The equivalent circuit is now in the Laplace transform domain, where $\hat{D}(s)$ and $\hat{V}(s)$ are the Laplace transforms of $\hat{d}(t)$ and $\hat{v}(t)$, respectively.

The procedure just outlined for the boost power stage is also applicable to the buck-boost power stage. The steady-state and perturbation components of the output voltage are easily derived for the buck-boost power stage from Figs. 11(a) and 11(b), respectively. The equivalent circuit for perturbations was linearized by Eq. (13), as before.

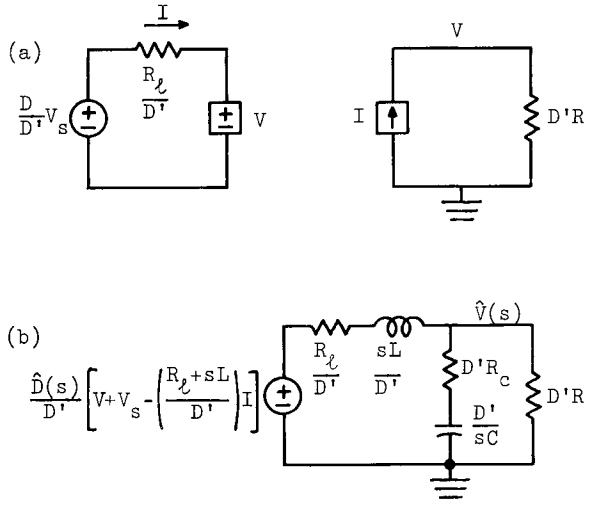

Figure 11. Equivalent circuits of the averaged buck-boost power-stage model for small control variations and a constant control: (a) steady state, and (b) linearized for variations.

Linearized equivalent circuits for small-amplitude control perturbations have been derived for each power stage. The factors which multiply $\hat{d}(s)$ in the equivalent voltage generators in Figs. 10(f) and 11(b) can be identified as the transfer function of an effective amplifier $A_c(s)$ as shown in Fig. 12; thus the linearized control-input transfer function $G_c(s)$,

$$G_c(s) \equiv \left.\frac{\hat{v}(s)}{\hat{d}(s)}\right|_{\text{zero initial conditions}} , \qquad (14)$$

for each power-stage type can be written in the form

$$G_c(s) = A_c(s)\, G_f(s) , \qquad (15)$$

where

$$A_c(s) = A_{co}(1 - s/\omega_a) , \qquad (16)$$

and $G_f(s)$ is the filter transfer function given by Eq. (7). Analytic expressions for the normalized filter and amplifier factors are contained in Table 1. The duty ratio has the same influence on effective component values as observed for source variations. Notice in addition the unusual form of the effective amplifier transfer function for boost and buck-boost power stages; the real zero is positive for $D' > D'_o$, where

$$D'_o = \begin{cases} \sqrt{\dfrac{R_\ell}{R}} , & \text{boost} \\ \sqrt{\left(1+\dfrac{R_\ell}{R}\right)\dfrac{R_\ell}{R}} - \sqrt{\dfrac{R_\ell}{R}} , & \text{buck-boost} \end{cases} . \qquad (17)$$

Since R_ℓ/R, and consequently D'_o, is typically small, ω_a is usually positive, so both the phase lag and amplitude of $A_c(j\omega)$ increase with ω. Figure 13 shows the block diagram of $G_c(s)$ in order to expose the similarity of interpretation of Eqs. (15) and (6).

Rather unusual analytical results have been derived from the averaged power stages. To the authors' knowledge, no tractable analysis of the transient or frequency response associated with a control variation has appeared in the literature

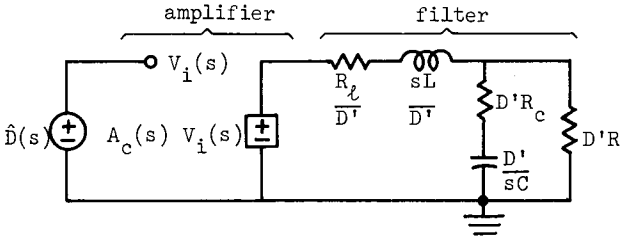

Figure 12. Equivalent circuit showing an effective amplifier in the averaged boost and buck-boost power-stage models for small control variations and a constant source.

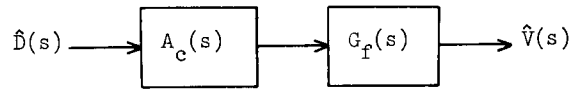

Figure 13. Linearized block diagram of the averaged power-stage model for small control variations and a constant source.

for boost or buck-boost power stages. However, Kossov (2) has performed an exact static analysis of the source-to-output gain for the three basic power stages, so for comparison the corresponding gains will be derived from the averaged power-stage models.

For static conditions expressed by Eqs. (3) and (8), the averaged power-stage models are particularly simple since there is no capacitor current or inductor voltage in the steady state. The static source-to-output gain of each power-stage configuration is easily derived (1):

$$V/V_s = \frac{D\,R}{R_\ell + R} , \quad \text{buck} \qquad (18)$$

$$V/V_s = \frac{D'\,R}{R_\ell + (D')^2 R} , \quad \text{boost} \qquad (19)$$

$$V/V_s = \frac{D\,D'\,R}{R_\ell + (D')^2 R} , \quad \text{buck-boost} . \qquad (20)$$

It may be observed that with corresponding notation Eqs. (18) to (20) agree precisely with Kossov's Eqs. (6a), (6b), and (6c).

Though not analytically founded, a hypothesis postulated by Wells et al. (5) states that the lowest corner frequency in the open-loop boost control-input describing function varies proportionately with D'. Wells' hypothesis was reportedly supported by experimental observations of a particular boost configuration with additional input and output filtering. The averaged model of the boost power stage under consideration here has a quadratic pole with break frequency ω_o given in Table 1 which does, in fact, vary approximately with D' for typical circuit values and operating conditions:

$$\omega_o \simeq \frac{D'}{\sqrt{LC}}\sqrt{\frac{R}{R + R_c}} \quad \text{for } D' \gg D'_o , \quad \text{boost} . \qquad (21)$$

To the extent that the effective source impedance (source impedance, input filter, and boosting inductor) is inductive and the effective load impedance (output filter and load) is capacitive, Wells' hypothesis may be a general result; notice, however, that the corner frequency of the effective amplifier is a stronger function of duty ratio:

$$\omega_a \simeq (D')^2\, R/L , \quad \text{for } D' \gg D'_o , \quad \text{boost} . \qquad (22)$$

OPEN-LOOP BEHAVIOR

Of the two input variations considered in the preceding section, responses to control variations are considerably more interesting because the averaged power-stage models are nonlinear with respect to control variations. Analog computer simulations (1) of the switched power stages in Fig. 2 and the corresponding averaged power stages in Fig 4 are subjected to transients and sinusoidal perturbations of the control for comparison with the analytic expressions just derived, but first a specific switch controller is chosen to operate the switched power stage.

Switch Controller

A pulse-width-modulator (PWM) is used to control the switches in the computer simulation of the power stages in Fig. 2. The PWM samples the controller input ϵ at uniform time intervals to initiate a sequence of output pulses whose durations are proportional to the sampled input values:

$$d(t) = \begin{cases} 1; & 0 \le t-nT < \tau_n \\ 0; & \text{otherwise} \end{cases} , \quad n = \text{integer}, \quad (23)$$

where

$$\frac{\tau_n}{T} = \begin{cases} 0; & \epsilon(nT) < 0 \\ \epsilon(nT); & 0 \le \epsilon(nT) < 1 \\ 1; & 1 < \epsilon(nT) \end{cases} , \quad n=\text{integer}. \quad (24)$$

To compare computer results with analysis, one should use a simple analytic controller model. Step changes of ϵ manifest themselves in the controller output within a switching period T and the controller output remains unchanged thereafter. Since T is much less than the response time of the power stage, the PWM does not significantly affect the overall transient response. Sinusoidal control perturbations are a different matter; however, if the dimensionless controller input, as shown in Fig. 14(a), is given by

$$\epsilon(t) = U + u \sin(\omega t - \phi) , \quad (25)$$

where $U+u<1$ and $U-u>0$, then the spectrum of the controller output shown in Fig. 14(b) can be evaluated by the extension (1) of a tedious two-dimensional Fourier analysis (6):

$$d(t) = U - \sum_{m=-\infty}^{\infty} \sum_{n=-\infty}^{\infty} e^{-jn(\phi+\pi)} \frac{J_n[u\Lambda T]}{j\Lambda T} e^{j\Lambda(t-UT)}$$

$$\Lambda \equiv m\omega_s + n\omega \neq 0$$

$$+ \sum_{\substack{m=-\infty \\ m\neq 0}}^{\infty} \frac{1}{jm\omega_s T} e^{jm\omega_s t} , \quad (26)$$

where $J_n[z]$ is a Bessel function of the first kind.

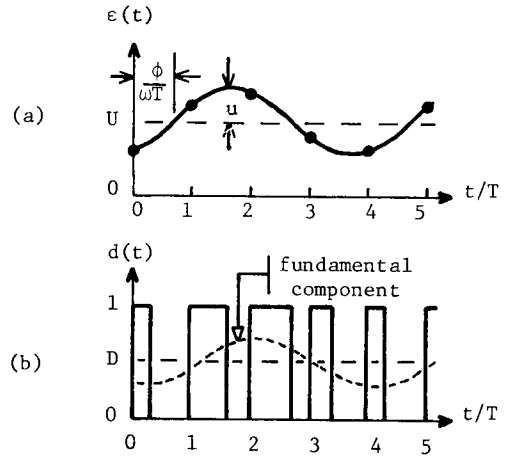

Figure 14. PWM response to sinusoidal modulation: (a) input, and (b) output.

Whether ω and ω_s are commensurable or not, the describing function of the PWM can be approximated well for small u by $\exp(-j\omega UT)$; thus the frequency response of the PWM can be modeled by a phase lag which increases linearly with modulation frequency ω.

Component Values

The following numerical values are consistent with typical design constraints ($L/R_\ell \gg T$, $RC \gg T$, $2L/R > T$) and will be used henceforth for specific analysis.

$$\left.\begin{aligned} T &= 10^{-4} \text{ second} \\ R &= 60 \text{ ohm} \\ L &= 6\cdot10^{-3} \text{ henry} \\ C &= 1/24\cdot10^{-3} \text{ farad} = 41.7\mu\text{f} \\ R_\ell &= 3 \text{ ohm} \\ R_c &= 1 \text{ ohm} \\ V_s &= 60 \text{ volt} \end{aligned}\right\} \quad (27)$$

Transient Response

It is convenient to record on a strip chart the transient response of switched and averaged converter models as simulated on the analog computer. Whereas step transitions of ϵ and $\langle d \rangle$ between all permutations of the levels 0.25, 0.50, and 0.75 were investigated, only representative transitions for the boost power stage are shown here. Figure 15 shows corresponding experimental transient responses of the switched and averaged models for comparison; the excellent correlation is typical of all power stages and control transitions. Notice qualitatively how the damping factor and natural frequency depend on duty ratio as predicted.

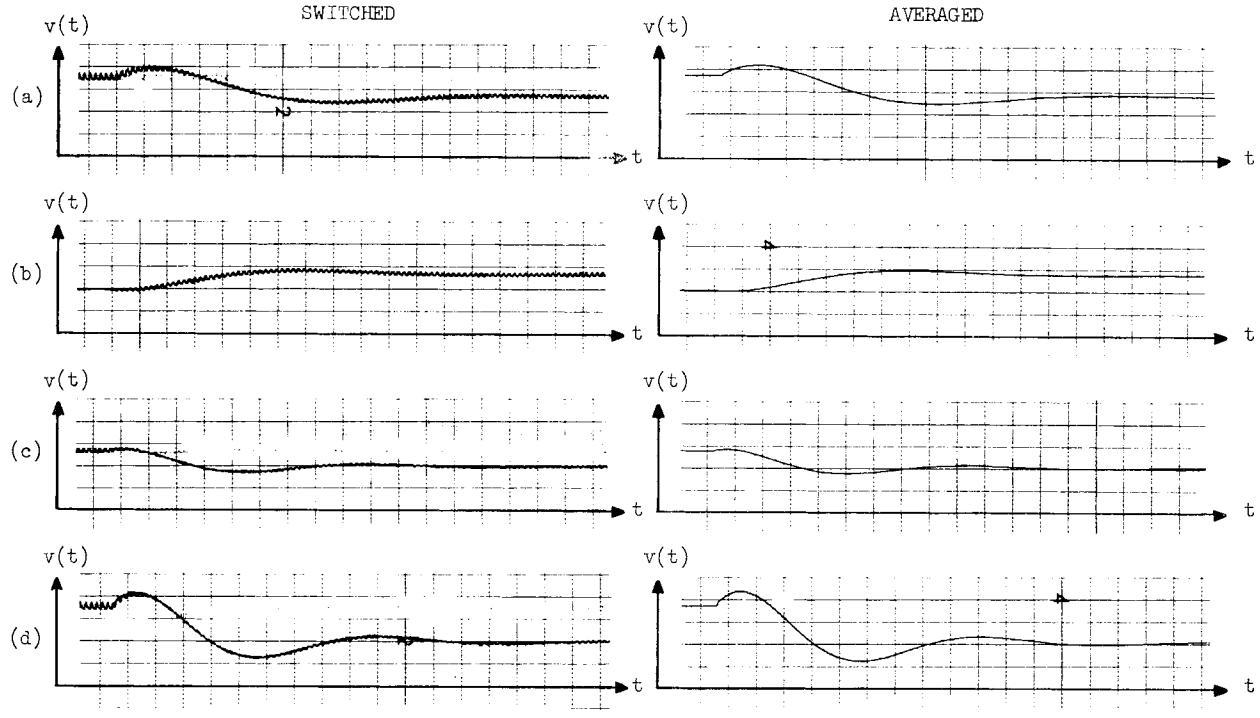

Figure 15. Experimental transient responses of switched and averaged boost power-stage models. Control transitions are (a) 0.75 → 0.50, (b) 0.25 → 0.50, (c) 0.50 → 0.25, and (d) 0.75 → 0.25; [scale factors: 36 v/Div vertical, 0.5 msec/Div horizontal].

Frequency Response

A simple analytic description of converter frequency response results when the PWM describing function is multiplied with the linearized control-input power-stage describing function $G_c(j\omega)$ in Eq. (15). A Bode plot of the theoretical frequency response of a boost converter is shown in Fig. 16 for several values of duty ratio.

Experimental frequency response is measured by enforcing a control input in the form of Eq. (25). At any given modulation frequency ω, the control input and power-stage output are simultaneously recorded on a strip chart, from which the amplitude and phase of the output component at the modulation frequency can be measured with respect to the modulation amplitude and phase. The amplitude and phase of the effective transfer function are then located on a Bode diagram. Figure 17 shows experimental data from the switched and averaged models of the boost power stage superimposed on the theoretical frequency response for D=0.50. The degree of correlation in evidence is typical of the other power stages and duty ratios investigated.

The scattering of switched data at higher frequencies in Fig. 17 leaves uncertain the role of various theoretical factors in determining the overall frequency response. To study this question one can decompose the theoretical transfer function into distinct factors which represent the effective amplifier, filter, and switch controller of the averaged boost power stage. These component factors[3], together with the composite response, are plotted as a function of frequency in Fig. 18 and show that data correlation with the computed curve in Fig. 17 would be much worse if any single theoretical factor were missing; in particular, the presence of the effective amplifier term, novel because of its real positive zero, has been confirmed.

[3]For convenient amplitude normalization, the scale factor V_s is divided from the amplifier factor and multiplied with the filter factor.

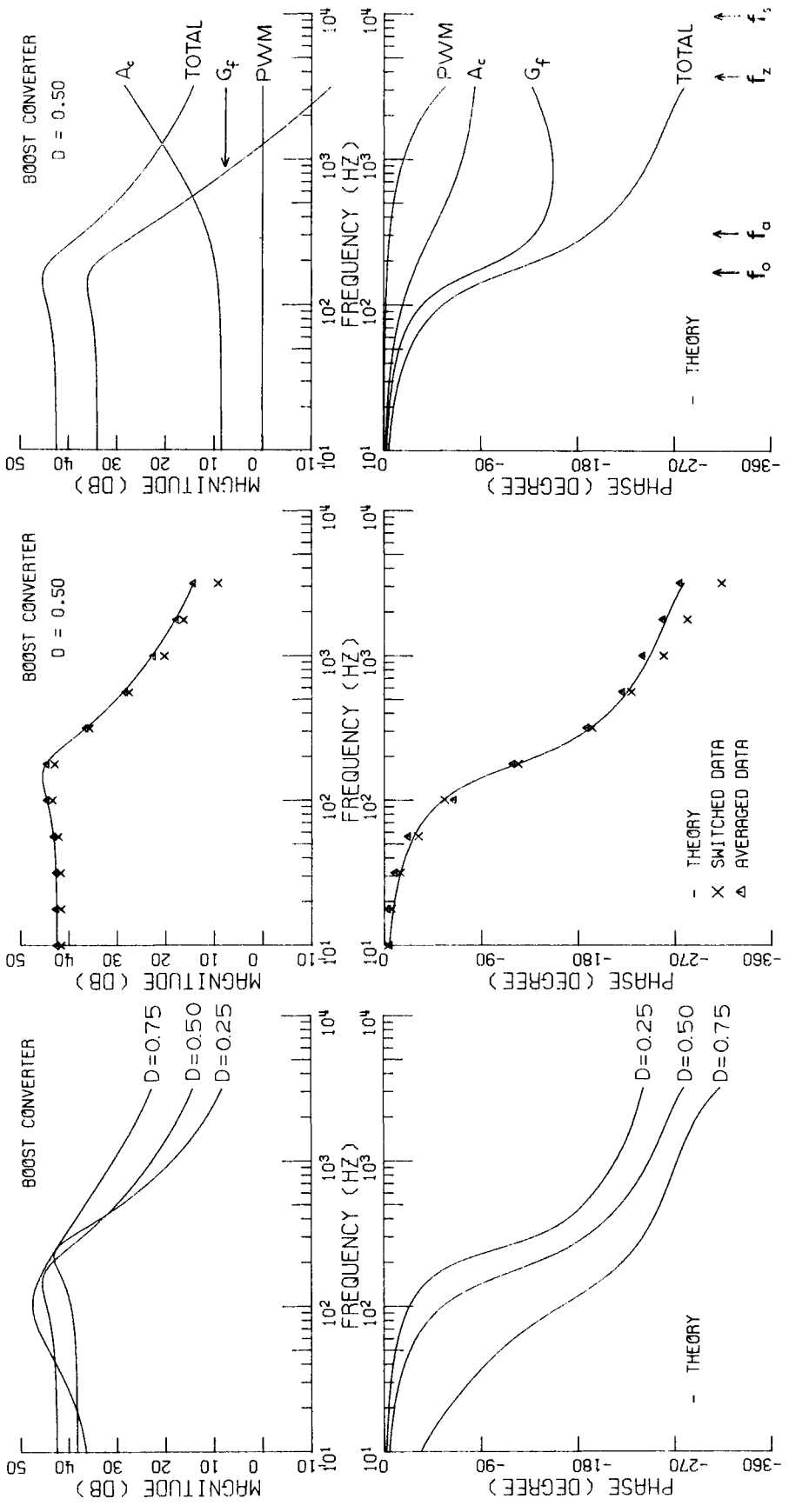

Figure 16. Theoretical control-input frequency response of the boost converter.

Figure 17. Experimental control-input frequency response of the boost converter for D = 0.50.

Figure 18. Components of the theoretical control-input frequency response of the boost converter for D = 0.50.

CLOSED-LOOP BEHAVIOR

Given that the open-loop frequency response of switched power stages is approximated by that of the averaged models, one should investigate how well the closed-loop behavior of the switched system can be predicted by the averaged system. One must remember that validity of stability predictions from the averaged model is inherently limited to frequencies less than the switching frequency. The objective of this section is to provide a comparison between theoretical closed-loop stability of averaged systems and experimental stability measurements of switched systems.

The feedback configuration used for stability analysis is shown in Fig. 19 and was designed to make the dc controller output independent of the feedback factor K. When K=0 (no feedback), the dc controller input U sets values for the static PWM output D and the static output voltage V; if V_r is chosen equal to V, then the static output voltage remains constant as K increases.

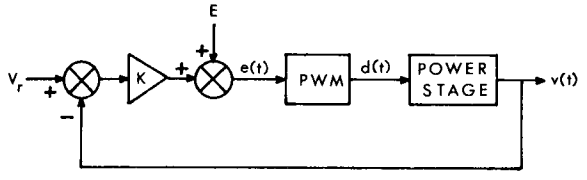

Figure 19. Converter in a closed-loop regulator configuration.

Local stability can be experimentally examined by gradually increasing the value of the gain factor K until a small disturbance in the steady-state limit cycle no longer decays with time but grows in amplitude. The critical value of K which separates the two modes of behavior is denoted K_c, and the corresponding oscillation occurs at frequency ω_c. Theoretical values for K_c and ω_c are computed from expressions for the frequency response of the averaged models by observing the frequency ω_c where the phase lag is π and then computing the gain factor K_c which makes the magnitude of the open-loop gain equal to unity.

Experimental values of K_c and ω_c are compared in Table 2 with predicted analytical values. Experimental values could not be obtained in the buck-boost simulation for D=0.25 because, as K increases, the discontinuities in output voltage, which are a consequence of switched current through the parasitic resistance of the imperfect filter capacitor, drive the switch controller into a saturated condition before the system becomes unstable; however, one should conclude from Table 2 that empirical closed-loop stability data from the switched simulation correlates well, overall, with values derived analytically from the averaged models.

Table 2 Critical stability factors of the closed-loop regulator configuration.

D	K_c		$\omega_c[10^3$ rad/sec]	
	Theory	Measured	Theory	Measured
Boost				
0.25	0.028	0.034	2.84	2.87
0.50	0.012	0.015	1.73	1.65
0.75	0.004	0.007	0.73	0.82
Buck-boost				
0.25	0.158	-	6.34	-
0.50	0.023	0.037	2.37	1.89
0.75	0.006	0.010	0.93	1.13

CONCLUSIONS

A technique to characterize the low-frequency response of switched power stages has been developed and applied to the simple analytic evaluation of source- and control-input describing functions. Analysis of continuous models which approximate the behavior of switched converters reveals several interesting characteristics including, for boost and buck-boost power stages, the modification of effective component values by the switch duty ratio, and the typical existence of a real positive zero in the linearized control-input describing function. The pulse-width-modulator as a switch controller exerts only weak influence on the frequency response in comparison with the power stage. The averaging technique can include parasitic effects such as realistic switch and diode models in the analysis. A computer simulation demonstrates that both open- and closed-loop responses of switched power stages are predicted well by continuous models; thus, the averaging technique should be a useful tool for the design and analysis of switched converters.

REFERENCES

(1) G. W. Wester, "Low-Frequency Characterization of Switched d-c Converters," Ph.D. thesis, California Institute of Technology, Pasadena, California, May 1972.

(2) O. A. Kossov, "Comparative Analysis of Chopper Voltage Regulators With LC Filter," IEEE Trans. Magnetics MAG-4, pp. 712-715, December 1968.

(3) L. R. Poulo and S. Greenblatt, "Research Investigations on Feedback Techniques and Methods for Automatic Control," Bose Corp., Natick, Mass., Contract ECOM-0520-F, pp. 156-165, April 1969.

(4) E. E. Landsman, "Modular Converters for Space Power Systems," Power Conditioning Specialists

Conf. Record, NASA Goddard Space Flight Center, Greenbelt, Md., pp. 87-99, April 20-21, 1970.

(5) B. A. Wells, B. T. Brodie, I. M. H. Bábaá, "Analog Computer Simulation of a dc-to-dc Flyback Converter," Supp. to IEEE Trans. Aerospace AES-3, pp. 399-409, November 1967.

(6) H. E. Rowe, Signals and Noise in Communications Systems, D. Van Nostrand Co., Inc., Princeton, N. J., pp. 257-280, 1965.